Super-Poissonian noise, negative differential conductance, and relaxation effects in transport through molecules, quantum dots, and nanotubes

Axel Thielmann,[1] Matthias H. Hettler,[1] Jürgen König,[2] and Gerd Schön[1,3]
[1]*Forschungszentrum Karlsruhe, Institut für Nanotechnologie, 76021 Karlsruhe, Germany*
[2]*Institut für Theoretische Physik III, Ruhr-Universität Bochum, 44780 Bochum, Germany*
[3]*Institut für Theoretische Festkörperphysik, Universität Karlsruhe, 76128 Karlsruhe, Germany*
(Received 25 June 2004; published 31 January 2005)

We consider charge transport through a nanoscopic object, e.g., single molecules, short nanotubes, or quantum dots, that is weakly coupled to metallic electrodes. We account for several levels of the molecule/quantum dot with level-dependent coupling strengths, and allow for relaxation of the excited states. The current–voltage characteristics as well as the current noise are calculated within first-order perturbation expansion in the coupling strengths. For the case of asymmetric coupling to the leads we predict negative-differential-conductance accompanied with super-Poissonian noise. Both effects are destroyed by fast relaxation processes. The nonmonotonic behavior of the shot noise as a function of bias and relaxation rate reflects the details of the electronic structure and level-dependent coupling strengths.

DOI: 10.1103/PhysRevB.71.045341 PACS number(s): 73.63.−b, 73.23.Hk, 72.70.+m

I. INTRODUCTION

The field of molecular electronics[1] is driven by the quest for functional electronic devices that are smaller than those produced by standard semiconductor technology. The microscopic size and the reproducibility in the production of molecules provide decisive advantages even if many, identical, molecules should be needed to build fault-tolerant devices. A negative differential conductance (NDC), a promising feature for functional devices, has been found recently in organic molecules.[2] Furthermore, many-body effects such as the Coulomb blockade and Kondo effect, known from semiconductor quantum dots,[3] have been observed in molecular devices[4,5] and carbon nanotubes.[6–8]

Since the typical single-particle level spacing of quantum dots (or short nanotubes) is small—often only a fraction of a meV—low temperatures are required for the resolution of transport through individual levels. Low temperatures are also helpful for the observation of quantum or shot noise. For example, at temperatures above 30 K noise transport through molecules between gold break junctions[9] appears to be dominated by $1/f$-like noise, believed to be generated by thermally induced fluctuations of the gold atoms. Such effects are suppressed at sub-Kelvin temperatures, at which the shot noise associated with the discreteness of the charge of the transfered electrons[10] can be detected. Both the current and the shot noise depend on details of the discrete level spectrum and the coupling strengths of these levels to the electrodes.[11–13] The combined measurements of current and shot noise, thus, provide a "spectroscopic" tool to gain information about the level structure.

Negative differential conductance through multilevel systems can occur when two adjacent levels have different coupling strengths to the leads. Once the level with weaker coupling is occupied, transport through the other level is suppressed, which reduces the total current. For molecules, it is well known that the coupling of different molecular orbitals to the electrodes may vary strongly due to differences in the spatial structure of the corresponding wave functions.[14] In metallic single-walled nanotubes (SWNTs), two bands cross the Fermi surface as the doping level is varied. For short tubes, these bands break up in a set of single-particle levels, separated by a level spacing δE of about 1 meV or less (see also Ref. 7 for multiwalled nanotubes). In general, these levels differ in their spatial structure and coupling strength, particularly if they are derived from two different bands at different points of the one-dimensional Brillouin zone. For semiconducting nanotubes similar considerations hold.[8] NDC has also been observed in semiconductor quantum dots.[15]

To study transport through systems which display a NDC, we start from an effective model of a few single-particle levels with couplings to the electrodes which vary strongly from level to level, and which also may differ for the source and drain electrodes. Furthermore, we include the possibility of relaxation among the levels: at finite bias voltage, electrons might enter the molecule (quantum dot or nanotube) at a high-lying excited state. Provided that the relaxation is fast as compared to the tunneling, the molecule might relax to the ground state or other low-lying state before the electron has the chance to leave the molecule. The relaxation is accompanied by the emission of a boson, either a photon or a phonon. Such relaxation processes can have a strong impact on the negative differential conductance by destroying the blocking mechanism.[14,16] Related models (without coupling to a bosonic bath and relaxation) were studied in Refs. 17–19.

The main purpose of this work is to study shot noise for the model described above in the regime where NDC might occur. We predict that in the absence of relaxation, the NDC is accompanied with super-Poissonian noise. This is formally similar to transport through semiconducting resonant tunneling devices,[20] though the origin of NDC in these devices (chemical potential passes through the semiconductor band edge) is entirely different from the one discussed here. Relaxation processes enhance the current and reduce the noise

in the NDC regime. The shot noise shows rather rich behavior depending on the coupling and relaxation strength. In particular, we find that the shot noise is a nonmonotonic function of the relaxation rate. This behavior contrasts with the current, which monotonically increases as the relaxation rate becomes larger. We are able to present analytic results for the shot noise, which might be useful for the interpretation of future experiments. We also relate our results to models of transport through several quantum dots.

II. THE MODEL

As a model for electron transport through a molecule or nanotube with M molecular orbitals (levels) and Coulomb interaction we consider a generalized Anderson impurity model coupled to a bosonic bath, described by the Hamiltonian $\hat{H}=\hat{H}_L+\hat{H}_R+\hat{H}_M+\hat{H}_{T,L}+\hat{H}_{T,R}+\hat{H}_{\rm ph}$ with

$$\hat{H}_r=\sum_{k\sigma}\epsilon_{k\sigma r}a^\dagger_{k\sigma r}a_{k\sigma r}, \tag{1}$$

$$\hat{H}_M=\sum_{l\sigma}\epsilon_{l\sigma}c^\dagger_{l\sigma}c_{l\sigma}+U\sum_l n_{l\uparrow}n_{l\downarrow}+E_c\left(\sum_{l\sigma}n_{l\sigma}\right)^2 \tag{2}$$

$$\hat{H}_{T,r}=\sum_{lk\sigma}(t^r_l a^\dagger_{k\sigma r}c_{l\sigma}+\text{h.c.}), \tag{3}$$

$$\hat{H}_{\rm ph}=\sum_q \omega_q d^\dagger_q d_q+\sum_{q,\sigma,l,l'}g^{l,l'}_q(d^\dagger_q+d_q)c^\dagger_{l\sigma}c_{l'\sigma}, \tag{4}$$

where $l=1,\ldots,M$ and $r=L,R$. Here, $\hat{H}_L$ and $\hat{H}_R$ model the noninteracting electrons with density of states $\rho_e=\Sigma_k\delta(\omega-\epsilon_{kr})$ in the left and right electrode ($a^\dagger_{k\sigma r}$, $a_{k\sigma r}$ are the Fermi operators for the states in the electrodes). The molecule term $\hat{H}_M$ describes a "molecule" with M relevant molecular orbitals of energy $\epsilon_{l\sigma}$ and Coulomb interaction on the molecule ($c^\dagger_{l\sigma}$, $c_{l\sigma}$ are Fermi operators for the molecular levels, and $n_{l\sigma}=c^\dagger_{l\sigma}c_{l\sigma}$ is the number operator). The charging energy E_c accounts for the classical energy cost to add charge on a confined system with many electrons and ions that are not explicitly considered in the Hamiltonian. It is the standard term for accounting for the effects of Coulomb repulsion between electrons in orbitals with large spatial extent, as realized in quantum dots and nanotubes. In addition, the Hubbard-like term with energy U punishes double occupancy within the same orbital. This is most relevant for more localized orbitals as realized in small molecules. The two kinds of interaction terms are the most important parts of the full two-body interactions present in a real molecule (quantum dot, nanotube). Other terms could be considered by much more elaborate models, as done in Ref. 21 for the computation of the $I-V$ characteristics. For the NDC/relaxation effects on the shot noise that we wish to study, the above simple molecule model suffices. According to which physical system (molecule, quantum dot, or nanotube) one wishes to describe, the parameters of the model can be suitably chosen.

Tunneling between leads and molecule levels is modeled by $\hat{H}_{T,L}$ and $\hat{H}_{T,R}$. The coupling strength is characterized by the intrinsic linewidth $\Gamma^r_l=2\pi|t^r_l|^2\rho_e$, where t^r_l are the tunneling matrix elements. In order to allow for relaxation between different molecular levels, we add $\hat{H}_{\rm ph}$, which describes a bosonic bath (where $d^\dagger_q$, d_q are the corresponding Bose operators) coupled to the molecule by the coupling constants $g^{l,l'}_q$, $l\neq l'$. This allows relaxation processes where electrons on the molecule can change the orbital by emitting or absorbing a boson. Note that a diagonal coupling, $l=l'$, would not be associated with relaxation but would give rise to "boson-assisted tunneling" leading to additional steps in the $I-V$ characteristics when the boson bath has a discrete spectrum.[22–24] Since in the present paper we are not interested in those boson-assisted tunneling processes, we take into account off-diagonal coupling contributions only. To be specific, we assume in the following that the bosonic bath consists of photons, although vibrational effects due to phonons could also be described within our model. For simplicity, we assume the constants $g^{l,l'}_q=(1-\delta_{l,l'})g_{\rm ph}$ to be independent of l,l', and q, and introduce the coupling $\alpha_{\rm ph}$ as $\alpha_{\rm ph}(\omega)=2\pi g^2_{\rm ph}\rho_b(\omega)$, where $\rho_b(\omega)=\Sigma_q\delta(\omega-\omega_q)$ is the density of states of the bosonic bath. For the relaxation due to photons we choose a power law behavior $\rho_b(\omega)\propto\omega^3$, corresponding to photons with three spatial degrees of freedom. For the case of phonon-mediated relaxation, which we are not going to discuss in detail in the present paper, the density of states is sharply peaked around the vibration modes of the molecule. The above model is an extension of the Anderson impurity model with one level (and in the absence of relaxation effects), which was described and discussed in Ref. 12.

We are interested in transport through the molecule, in particular in the current I and the (zero-frequency) current noise S. They are related to the current operator $\hat{I}=(\hat{I}_R-\hat{I}_L)/2$, with $\hat{I}_r=-i(e/\hbar)\Sigma_{lk\sigma}(t^r_l a^\dagger_{k\sigma r}c_{l\sigma}-\text{h.c.})$ being the current operator for electrons tunneling into lead r, by $I=\langle\hat{I}\rangle$ and

$$S=\int_{-\infty}^{\infty}dt\langle\delta\hat{I}(t)\delta\hat{I}(0)+\delta\hat{I}(0)\delta\hat{I}(t)\rangle \tag{5}$$

where $\delta\hat{I}(t)=\hat{I}(t)-\langle\hat{I}\rangle$.

III. DIAGRAMMATIC TECHNIQUE

For the calculation of the current I and current noise S, we use the diagrammatic technique developed in Ref. 24 and expanded for the description of the noise in Ref. 12. In lowest-order perturbation theory in the coupling strengths Γ^r_l, the following expressions for the current and the noise were found:

$$I=\frac{e}{2\hbar}\mathbf{e}^T\mathbf{W}^I\mathbf{p}^{\rm st}, \tag{6}$$

$$S=\frac{e^2}{\hbar}\mathbf{e}^T(\mathbf{W}^{II}\mathbf{p}^{\rm st}+\mathbf{W}^I\mathbf{P}\mathbf{W}^I\mathbf{p}^{\rm st}). \tag{7}$$

The boldface indicates matrix notation related to the molecular state labels χ (for the M level system there are 4^M differ-

ent states). The vector $\mathbf{e}$ is given by $e_\chi=1$ for all χ. The zeroth-order stationary probabilities $\mathbf{p}^{\rm st}$ can be expressed in terms of first-order transition rates $W_{\chi,\chi'}$ (forming a matrix $\mathbf{W}$) between two molecular states χ and χ' as

$$\mathbf{p}^{\rm st}=(\tilde{\mathbf{W}})^{-1}\mathbf{v}. \tag{8}$$

The matrix $\tilde{\mathbf{W}}$ is identical to $\mathbf{W}$ but with one (arbitrarily chosen) row χ_0 being replaced with $(\Gamma,\ldots,\Gamma)$. Then the vector $\mathbf{v}$ is given by $v_\chi=\Gamma\delta_{\chi\chi_0}$. The total transition rates $W_{\chi,\chi'}$ (in the absence of relaxation) are the sum of transition rates associated with electron tunneling through either the left or the right barrier, $W_{\chi,\chi'}=W^R_{\chi,\chi'}+W^L_{\chi,\chi'}$.

The matrix elements of $\mathbf{W}^I$ and $\mathbf{W}^{II}$ are given by $W^I_{\chi,\chi'}=(W^R_{\chi,\chi'}-W^L_{\chi,\chi'})[\Theta(N_{\chi'}-N_\chi)-\Theta(N_\chi-N_{\chi'})]$ and $W^{II}_{\chi,\chi'}=\frac{1}{4}(W^R_{\chi,\chi'}+W^L_{\chi,\chi'})(1-2\,\delta_{\chi\chi'})$, where N_χ is the total number of electrons on the molecule within the state χ. The indices *I* or *II* indicate that one or two vertices in the corresponding diagram are due to current operators present in the definition for the current *I* and the noise *S*.

The matrix $\mathbf{P}$ is associated with the propagation between two blocks $\mathbf{W}^I$ containing one current operator each. To lowest order in Γ,

$$\mathbf{P}=(\tilde{\mathbf{W}})^{-1}\mathbf{Q} \tag{9}$$

with $Q_{\chi'\chi}=(p^{\rm st}_{\chi'}-\delta_{\chi',\chi})(1-\delta_{\chi',\chi_0})$, i.e., $\mathbf{P}$ is of order Γ^{-1}, thus leading to a nonvanishing contribution of the second part in Eq. (7) even in lowest (first) order perturbation theory in the coupling to the electrodes. Similar expressions for the calculation of current and noise were derived by other means by Hershfield *et al.* in Ref. 25 and Korotkov in Ref. 26.

In order to include relaxation processes, we need to extend the theory of Ref. 12 by introducing corresponding transition rates $W^{\rm ph}_{\chi,\chi'}$. Assuming weak coupling to the bosonic bath (in addition to weak tunneling), we only keep contributions to either first order in $\alpha_{\rm ph}$ or to first order in Γ. The total transition rates are, thus, given by $W_{\chi,\chi'}=W^L_{\chi,\chi'}+W^R_{\chi,\chi'}+W^{\rm ph}_{\chi,\chi'}$, where $W^{\rm ph}_{\chi,\chi'}$ describe pure relaxation while $W^L_{\chi,\chi'}$ and $W^R_{\chi,\chi'}$ model pure tunneling. We have

$$W^r_{\chi',\chi}=2\pi\rho_e\sum_\sigma f^+_r(E_{\chi',\chi})\left|\sum_l t^r_l\langle\chi'|c^\dagger_{l\sigma}|\chi\rangle\right|^2+f^-_r(-E_{\chi',\chi})\times\left|\sum_l t^r_l\langle\chi'|c_{l\sigma}|\chi\rangle\right|^2 \tag{10}$$

for $\chi'\neq\chi$, together with $W^r_{\chi,\chi}=-\Sigma_{\chi'\neq\chi}W^r_{\chi',\chi}$. $E_{\chi',\chi}=E_{\chi'}-E_\chi$ is the energy difference between the many-body states χ and χ'. Here, $f(x)=1/[\exp(x/T)+1]$ is the Fermi function, $f^+(x)=f(x)$ and $f^-(x)=1-f(x)$, and $f^\pm_r(x)=f^\pm(x-\mu_r)$. The bosonic rates are

$$W^{\rm ph}_{\chi',\chi}=\sum_\sigma b(E_{\chi',\chi})\left|\sum_{l\neq\bar{l}}\langle\chi'|c^\dagger_{l\sigma}c^-_{l\sigma}|\chi\rangle\right|^2 \tag{11}$$

for $\chi'\neq\chi$, and $W^{\rm ph}_{\chi,\chi}=-\Sigma_{\chi'\neq\chi}W^{\rm ph}_{\chi',\chi}$, where $b(x)=\mathrm{sgn}(x)\alpha_{\rm ph}(x)n_b(x)$, with the Bose function $n_b(x)=1/[\exp(x/T)-1]$. While the presence of relaxation leads to a modification of $\mathbf{p}^{\rm st}$ and $\mathbf{P}$, the matrices $\mathbf{W}^I$ and $\mathbf{W}^{II}$ are not affected.

The rules for calculating the irreducible blocks $\mathbf{W}$ describing electron tunneling and relaxation are as follows.

(1) For a given order k draw all topologically different diagrams with $2k$ vertices connected by k tunneling (electron) lines or boson (photon) lines (for orders $k\geqslant 2$ both kinds of lines might be contained in a diagram). Assign the energies E_χ to the propagators, and energies $\omega_l(l=1,\ldots,k)$ to each one of these lines.

(2) For each of the $(2k-1)$ segments enclosed by two adjacent vertices there is a resolvent $1/(\Delta E_j+i0^+)$ with $j=1,\ldots,2k-1$, where ΔE_j is the difference of the left-going minus the right-going energies.

(3) Each vertex containing dot operators B_n (with n different operator structures) gives rise to a matrix element $\langle\chi'|B_n|\chi\rangle$, where $\chi(\chi')$ is the dot state entering (leaving) the vertex with respect to the Keldysh contour (for our model we have: $B_1=c^\dagger_{l\sigma}$, $B_2=c_{l\sigma}$, $B_3=c^\dagger_{l\sigma}c^-_{l\bar{\sigma}}$).

(4) The contribution of a tunneling line of reservoir r is $\gamma^\pm_{rl\sigma}(\omega_l)=\Gamma^l_r/2\pi\, f^\pm(\omega_l-\mu_r)$, taking the plus sign if the line is going backward with respect to the closed time path, and the minus sign if it is going forward. The same way the contribution of a bosonic line is given by $b(\pm\omega_l)=\mathrm{sgn}(\omega_l)\alpha_{\rm ph}(\omega_l)n_b(\pm\omega_l)$.

(5) There is an overall prefactor $(-i)(-1)^c$, where c is the total number of vertices on the backward propagator plus the number of crossings of tunneling lines (no bosonic lines) plus the number of vertices connecting the state d with $\uparrow$.

(6) Integrate over the energies ω_l of the tunneling and boson lines and sum over all reservoir and spin indices.

IV. RESULTS

In the following we discuss current and shot noise for the model of Eqs. (1)–(4) with two single-particle levels ($M=2\to l=1,2$) in first order perturbation theory in the tunnel couplings Γ^r and the coupling $\alpha_{\rm ph}$ to the bosonic bath. We express the different coupling parameters Γ^r_l, $\alpha_{\rm ph}$ in units of a scale Γ that has the same order of magnitude as the largest of the tunnel couplings Γ^r_l. (In the case of equal tunnel couplings, the natural choice is $\Gamma^R_1=\Gamma^L_1=\Gamma^R_1=\Gamma^L_2=\Gamma$.) Our perturbation expansion is valid for temperatures larger than the tunnel couplings. Throughout this paper, we choose $k_{\rm B}T=10\Gamma$. The molecule can acquire 16 possible states, as each level can be either unoccupied, occupied with spin $\uparrow$ or $\downarrow$, or doubly occupied. The system described is characterized by level energies ϵ_1 and ϵ_2, the "Hubbard" repulsion U, and the charging energy E_c. Furthermore, the electron and photon reservoirs have temperature T (set as $T=0.05$ meV) and are connected to the molecule via the coupling parameters Γ^r_l and $\alpha_{\rm ph}$.

Transport is achieved by applying a bias voltage $V_{\rm bias}$, which is dropped symmetrically at the electrode-molecule tunnel junctions, meaning that the energies of the molecular states are independent of the applied voltage even if the couplings Γ^r_l are not symmetric. The shape of potential profile (size of potential drops) is governed by the electrostatic Poisson equation, i.e., the capacitances of the molecule to the left

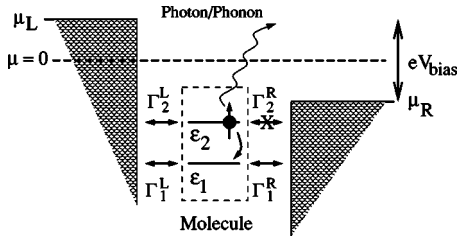

FIG. 1. Sketch of the couplings and processes in the considered model.

and right electrodes. In the weak coupling limit that we consider here, modifications of the couplings do not effect the potential profile. The effects of asymmetric voltage drop and a possible gate voltage are straightforward to anticipate, but would only obscure the results presented below.

An illustration of the transport situation is shown in Fig. 1. The Fano factor, which is given by the noise-to-current ratio, $F=S/2eI$, provides additional information about transport properties not contained in the current–voltage characteristics alone. Therefore we are interested in studying its dependence on different couplings to the electrodes, the strength of relaxation, the Coulomb charging energy, etc. in order to make predictions of the importance of those parameters for a given experiment.[27]

We focus on the easiest case which exhibits NDC. The set of energy parameters $\{\epsilon_1=-0.5$ meV, $\epsilon_2=0.5$ meV, $U=1.5$ meV, $E_c=1$ meV$\}$[28] describes a molecule that is uncharged at zero bias, as the energy to occupy the first single particle level is $\epsilon_1+E_c=0.5$ meV (state D_1). Without coupling to the boson bath and in contrast to the one level system discussed in Ref. 12 we find a negative differential conductance (NDC) regime, see Fig. 2, in dependence on the different coupling strength between the molecular orbitals and the reservoirs, as was previously discussed in Refs. 14, 16, and 17. The shot noise behaves qualitatively similar, the important quantitative details are discussed in the following.

If we chose equal tunnel coupling, $\Gamma_l^r=\Gamma$ (solid line), we find that current and shot noise S increase, each time, as a

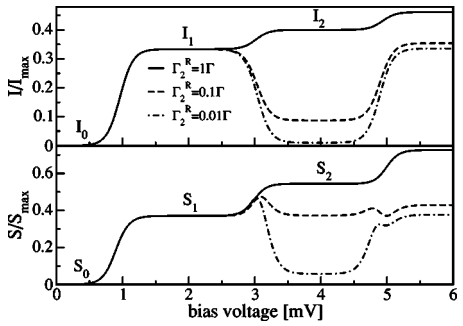

FIG. 2. Current I and shot noise S vs voltage for $k_BT=0.05$ meV, $\epsilon_1=-0.5$ meV, $\epsilon_2=0.5$ meV, $U=1.5$ meV, $E_c=1$ meV, symmetric bias ($\mu_L=-\mu_R=eV/2$), and $\Gamma_1^L=\Gamma_2^L=\Gamma_1^R=\Gamma$. The height of the plateaus labeled by $i=0$, 1, 2 are discussed in the text and depend on the choice of the coupling parameters. For suppressed coupling Γ_2^R current and shot noise break down leading to negative differential conductance (NDC) at a threshold energy. The curves are normalized to $I_{\max}=(e/\hbar)2\Gamma$ and $S_{\max}=(e^2/\hbar)2\Gamma$, respectively.

new transport "channel" (controlled by the excitation energies) opens. This leads to plateaus, separated by thermally broadened steps. The first four plateaus are shown and discussed in the following. At a bias voltage of 1 mV, sequential transport through the state D_1 with one electron on the lower lying level becomes possible. At 3 mV, additional transport through the D_2 state opens up, with the upper level being occupied with one electron. The different regions of interest are labeled by I_i, S_i with $i=0$, 1, 2. For a bias voltage above 5 mV, transport channels with two or more electrons on the molecule open up. In the large-bias regime (not indicated in the plots) and for symmetric coupling, the values $I_{\max}=(e/\hbar)2\Gamma$ and $S_{\max}=(e^2/\hbar)2\Gamma$ are reached. If now the coupling parameter Γ_2^R is suppressed with respect to the other couplings, this leads to suppressed curves for the current and shot noise in region 2, resulting in NDC at the threshold of 3 mV, when the state D_2 becomes relevant, see in Fig. 2 for $\Gamma_2^R=0.1\Gamma$ and 0.01Γ. The reason for the NDC is a combination of the Pauli principle, Coulomb blockade, and suppressed coupling, as discussed in Refs. 14,21. In our case, an electron, entering the upper molecular orbital from the left electrode, cannot leave the molecule if the coupling of this orbital to the right electrode is entirely suppressed. Transport through the lower molecular orbital is also not possible, since the simultaneous occupation of both orbitals is energetically forbidden in the considered bias regime. The electron gets stuck in the upper molecular orbital blocking other electrons from tunneling through the molecule. Consequently, the current collapses.

Since in lowest-order perturbation theory in Γ the plateau *heights* are given by the coupling parameters only, we find that for $\Gamma_2^R<2/3\Gamma$ NDC can be observed, whereas the shot noise is suppressed below its lower bias plateau only if $\Gamma_2^R<0.1\Gamma$. This difference can already give a rough idea about the coupling strength Γ_2^R for a given set of current and noise measurements. If the shot noise is sufficiently suppressed in the NDC region, a peak in the shot noise appears around the resonance energy of the second level. This peak is due to temperature induced fluctuations that in certain situations enhance the shot noise over the surrounding plateau values (where temperature fluctuations are exponentially suppressed). As the resonance is approached from lower bias, within the range of temperature broadening, the noise "detects" the opening of the second transport channel and increases. If the bias is beyond the resonance, the redistribution of occupation has taken place and the noise is algebraically suppressed. The result is the observed peak with width of the temperature. However, the peak height is only determined by the coupling parameters and is independent of the temperature. The current never shows such a peak, as it decreases proportional to the loss of occupation of the first level, the transport channel with "good" coupling.

The effect of NDC on the Fano factor, which is given by $F=S/2eI$, is shown in Fig. 3. At small bias, $eV\ll k_BT$, the noise is dominated by thermal noise, described by the well known hyperbolic cotangent behavior which leads to a divergence of the Fano factor.[10,29] The plateau for bias voltages below 1 mV (region 0) corresponds to the Coulomb blockade regime, where transport is exponentially suppressed. In the regions 1 (2) transport through the state $D_1(D_2)$ is possible.

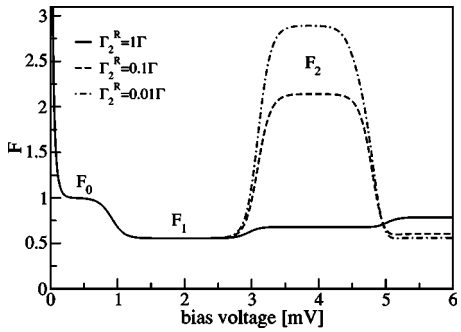

FIG. 3. Fano factor F vs bias voltage for the same parameters as in Fig. 2 and various coupling parameters Γ_2^R. The NDC effect results in a super-Poissonian value for the Fano factor.

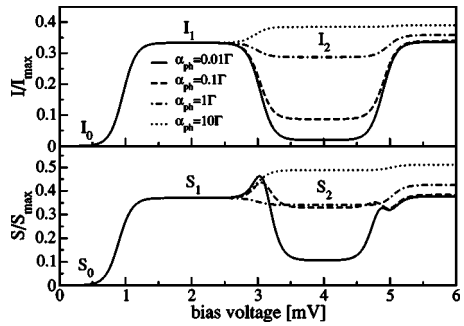

FIG. 4. Current I and shot noise S vs voltage for the same parameters as in Fig. 2 but fixed coupling $\Gamma_2^R=0.01\Gamma$. Coupling to a bosonic bath allows for relaxation processes. The coupling parameter α_{ph} is varied relative to Γ. The NDC effect is destroyed by strong relaxation.

The suppressed coupling strength Γ_2^R does not affect the plateau height F_1, whereas F_2 reaches values larger then 1, and up to 3.[17] This "super-Poissonian" noise ($F>1$) is predicted for $\Gamma_2^R<0.44\Gamma$. If the bias is larger than 5 mV tunneling through states is allowed where both orbitals are occupied simultaneously, i.e., the molecule can be doubly occupied. The Fano factor is sub-Poissonian again ($F<1$) in this regime. Comparing Figs. 2 and 3 graphically allows one to determine roughly the strength of the suppression of Γ_2^R. In general, however, depending on the underlying energy parameters (giving the ordering of a sequence of plateaus) and the coupling parameters (giving their height) other values for the Fano factor are possible. In the Coulomb blockade regime (region 0), for example, there can also be super-Poissonian noise, if both energy levels are below the equilibrium Fermi energy. Super-Poissonian noise is also possible for a single Anderson level, if the spin degeneracy is lifted by a magnetic field (in the Coulomb blockade regime) or by ferromagnetic leads, see Refs. 30,31. The energy and coupling parameters can be fully determined only by considering several transport regimes, e.g., by application of a gate voltage.

It should be noted that the nonmonotonic behavior of the Fano factor in regions 1 and 2 is entirely due to the second term of the noise expression Eq. (7) that accounts for "propagation" (and transitions) of molecular states between the two current vertices at different times.[17] On the plateaus of regions 1 and 2 the first term of Eq. (7) is always (i.e., for any coupling/relaxation parameter values) identical to the current times the electric charge e. Therefore it contributes a term $1/2$ to the Fano factor $F=S/2eI$.

Let us consider next the effect of relaxation processes on the current and shot noise curves. In Fig. 4 we keep the same set of energy parameters as in Fig. 2 and fix the coupling strength Γ_2^R at 0.01Γ suppressed relatively to the other molecule-electrode couplings. Now a parameter α_{ph} describes the coupling of the molecule with a boson bath. A value of $\alpha_{\mathrm{ph}}=0.01\Gamma$ is below even the relatively weak dipole coupling of photons to molecule states of small aromatic molecules such as benzene.[21] For this small photon coupling (solid line) current and shot noise are still reduced in region 2 relative to the plateau heights $I_1=1/3$ and $S_1=10/27$ in region 1. If now α_{ph} increases, we find that both I and S also increase in the NDC region, at least initially. If the value $\alpha_{\mathrm{ph}}=2\Gamma$ is exceeded, the NDC is gone (see also Fig. 6, dashed line). The behavior of the shot noise peak at the resonance energy is now further complicated by the effect of relaxation. The noise value at the resonance energy is nonmonotonic, i.e., it first decreases and then increases again with increasing relaxation. This is due to redistribution of occupation by the relaxation processes in favor of the first level.

For our chosen parameters, the value $\alpha_{\mathrm{ph}}=2\Gamma$ is larger than a reasonable molecule-photon coupling. However, phonon (vibrational) couplings could easily be strong enough to achieve such fast relaxation. On the other hand, molecule vibrations have a discrete spectrum, much different to the power law assumed in our calculations. Relaxation due to phonons can be only effective if the energies of a phonon and the electronic excitation match within the smearing provided by temperature. This obviously depends on the details of the molecule and cannot be discussed within the model considered here. The destruction of NDC by bosonic transition rates is easily explained. An electron which formerly was stuck on the upper molecular orbital can now relax onto the lower molecular orbital, from which tunneling to the right electrode is possible via the coupling Γ_1^R.

For the Fano factor in Fig. 5 an increase of α_{ph} leads to a decreasing value for the plateau F_2, which passes the Poissonian value $F=1$ at $\alpha_{\mathrm{ph}}\sim 0.34\Gamma$. Different to the current,

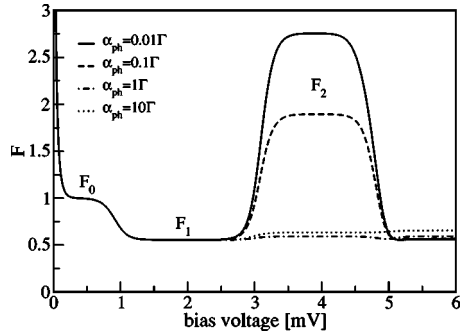

FIG. 5. Fano factor vs bias voltage for the same parameters as in Fig. 4 and various couplings to a bosonic bath α_{ph}. The super-Poissonian value of the Fano factor vanishes due to strong relaxation processes.

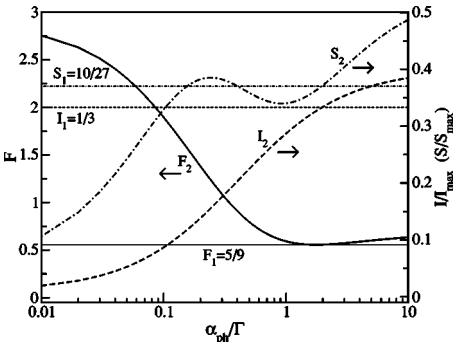

FIG. 6. Fano factor (left axis), current, and shot noise (right axis) vs coupling to the bosonic bath for the same set of parameters as in Fig. 4 and 5. The values I_1, S_1, F_1 of the first plateau do not depend on the bosonic coupling parameter, whereas on the second plateau (NDC region) both the shot noise and the Fano factor show a nonmonotonic dependence.

however, the Fano factor does not show monotonic behavior with increasing $\alpha_{\rm ph}$. The dashed-dotted line corresponding to $\alpha_{\rm ph}=1\Gamma$ lies below the dotted one with $\alpha_{\rm ph}=10\Gamma$. The nonmonotonic behavior is even more pronounced for the shot noise. It has a maximum and a minimum for $0.2\sim\alpha_{\rm ph}/\Gamma\sim 1$ before increasing again at $\alpha_{\rm ph}>\Gamma$, see Fig. 6. The richness of the noise behavior in the NDC regime might allow a detailed determination of coupling-parameter values.

Contrary to the (monotonic) $\alpha_{\rm ph}$-dependence of the current, which can be explained by a redistribution of occupation probability from the "blocking" upper level to the "conducting" lower level, it is difficult to present a simple physical picture for the nonmonotonic shot noise behavior in the NDC region. As noted above, it is the second term of the noise expression Eq. (7) that is responsible for variation of the noise with coupling parameters. For our set of parameters, the second term of Eq. (7) has a peak at about $\alpha_{\rm ph}\sim 0.16\Gamma$ and a minimum at $\alpha_{\rm ph}\sim 1.66\Gamma$, where it almost reaches zero. The increase of this term at small $\alpha_{\rm ph}$ is again explained by the lifting of the blockade, i.e., the redistribution of occupation probability. The decrease after the maximum is the result of a (near) cancellation of contributions from the different states participating in transport. Some of the state contributions are negative and counter the positive contributions that produce the maximum. Such a nonmonotonicity with coupling parameters is only possible (in first order perturbation theory) for a reducible observable like the shot noise, where aside from the stationary occupation probabilities the "molecule propagator" [in the form of **P** of Eq. (9)] also plays an important role.

Since in lowest-order perturbation theory temperature only leads to a thermal broadening of the steps, the plateau heights in the different transport regimes are given by the coupling parameters, both the tunnel coupling as well as the relaxation strength. However, note that the actual relaxation *rate* depends also on the position of the energy levels via the boson density of states. This will complicate matters in the general case with many levels, which are not equidistant from each other. In our case with two levels, we can extract analytical expressions for the plateau values current, noise, and Fano factor within the low bias transport regimes as indicated in Figs. 2–5. We find for the plateau of the NDC-region 2 ($S_2=2I_2F_2$)

$$I_2=\frac{\Gamma_1^R(\alpha_{\rm ph}+\Gamma_2^R)(\Gamma_1^L+\Gamma_2^L)/\Gamma}{2\Gamma_2^L(\alpha_{\rm ph}+\Gamma_1^R)+(2\Gamma_1^L+\Gamma_1^R)(\alpha_{\rm ph}+\Gamma_2^R)} \tag{12}$$

for the current and

$$F_2=\frac{\alpha_{\rm ph}(\alpha_{\rm ph}+2\Gamma_2^R)[(\Gamma_1^R)^2+4(\Gamma_1^L+\Gamma_2^L)^2]+[8\Gamma_1^L\Gamma_2^L(\Gamma_1^R-\Gamma_2^R)^2+4(\Gamma_1^L\Gamma_2^R+\Gamma_2^L\Gamma_1^R)^2+(\Gamma_1^R\Gamma_2^R)^2]}{[2\Gamma_2^L(\alpha_{\rm ph}+\Gamma_1^R)+(2\Gamma_1^L+\Gamma_1^R)(\alpha_{\rm ph}+\Gamma_2^R)]^2} \tag{13}$$

for the Fano factor. Since only bosonic transition between singly occupied levels 1 and 2 are possible in this bias region, the above expressions include only one bosonic rate $\alpha_{\rm ph}(\Delta E=\epsilon_2-\epsilon_1)$. Since the temperature is much smaller than ΔE, only relaxation processes matter for the plateau values. For completeness, we also give the expressions for the transport regime 1 (transport through the lower level only). They can be found from the above by setting the couplings Γ_2^L and $\alpha_{\rm ph}$ equal to 0. Then electrons can never enter the upper level at positive bias, leading to an effective one level system with the result[12]

$$I_1=\frac{2\Gamma_1^R\Gamma_1^L}{(2\Gamma_1^L+\Gamma_1^R)2\Gamma};\quad F_1=\frac{4(\Gamma_1^L)^2+(\Gamma_1^R)^2}{(2\Gamma_1^L+\Gamma_1^R)^2}. \tag{14}$$

The derivation of analytical expressions in the low bias regime allows us a quick study of current, noise, and Fano factor for arbitrary coupling situations. For the special situation where $\Gamma_1^{L,R}=\Gamma-\Gamma_2^{L,R}$ and $\alpha_{\rm ph}=0$ the Fano factor F_2 is presented in a contour plot (see Fig. 7). This choice allows the coupling parameters to the left and right reservoir to vary (independently) between 0 and Γ, while having the sum of the couplings to each reservoir fixed. Although not all of the possible coupling situations can be visualized this way, the following features which can be extracted from this plot are valid in general: A super-Poissonian Fano factor $F>1$ can only be found if $\Gamma_1^R\neq\Gamma_2^R$ and additionally $\Gamma_1^L\neq 0$, $\Gamma_2^L\neq 0$. Furthermore, a Fano factor $F>3$ is possible only if $\Gamma_1^L\neq\Gamma_2^L$ besides the above conditions. In the absence of relaxation processes ($\alpha_{\rm ph}=0$) we can also find a point symmetry of F_2. This symmetry is broken if $\alpha_{\rm ph}\neq 0$, as adsorption and emission rates of bosons differ due to the boson occupation factors.

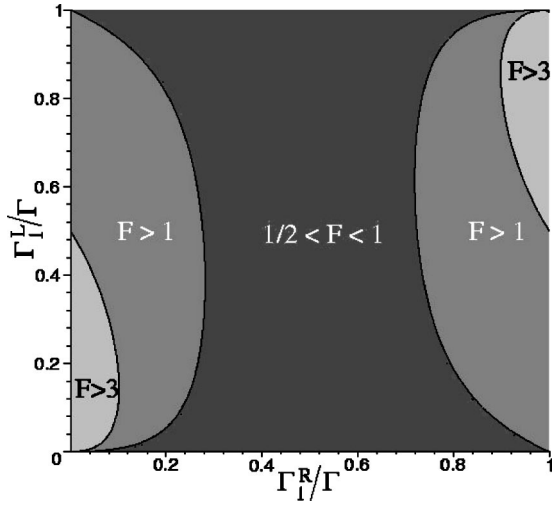

FIG. 7. Contour plot of the Fano factor (plateau F_2) with the choice $\Gamma_1^{L,R}=\Gamma-\Gamma_2^{L,R}$ and $\alpha_{\mathrm{ph}}=0$. The totally symmetric situation is given for $\Gamma_1^L=\Gamma_1^R=0.5\Gamma$. The Fano factor can become arbitrarily large if the system is sufficiently asymmetric.

The special case with the settings $\Gamma_l^L \to \Gamma_l^L/2$ describes spinless transport through a two-level system in the absence of relaxation processes. This situation was discussed in Ref. 19 where values of the Fano factor between $1/2$ and 3 were found in the case of equal couplings $\Gamma_1^L=\Gamma_2^L$. In the case $\Gamma_1^L \neq \Gamma_2^L$ we can even find Fano factors with values much larger than 3, as the shot noise is strongly enhanced compared to a current that is still sizable itself (not exponentially suppressed), see Fig. 7. This again only happens for a special set of coupling parameters, thus allowing a detailed analysis of the coupling parameters, if such high values for the Fano factor were observed in experiment.

Besides the super-Poissonian noise with Fano factors $F>1$ due to positive correlations and values between $1/2<F<1$ in the sub-Poissonian regime, we can also find values of coupling parameters in which the Fano factor drops to values below $1/2$. This behavior, however, can only be observed in the presence of relaxations, when the coupling strengths Γ_1^L and Γ_2^R are suppressed relative to the other tunnel couplings. If the above couplings are vanishing, there is only one path for the electrons to tunnel through the molecule, namely from the left electrode to the upper molecular orbital, then via relaxation onto the lower molecular orbital until finally the electrons leave the molecule by tunneling to the right electrode. By choosing specifically $\Gamma_1^L=\Gamma_2^R=0$ and $\Gamma_1^R=2\Gamma_2^L=\alpha_{\mathrm{ph}}$ the value of the Fano factor can be minimized and is found to be $1/3$. The probabilities to find an unoccupied molecule or an occupied molecule with one electron in the lower level doublet or in the upper level doublet are all equal in this case ($P_0=P_{D_1}=P_{D_2}=1/3$). This special situation reminds us of a system where a chain of quantum dots are coupled in series, having interdot tunnel couplings of the same size as the couplings of the chain ends to the leads. For an infinite chain of such dots (effectively a one-dimensional wire) the Fano factor also reaches $1/3$.[32,33]

In summary, we have discussed the interplay of Coulomb interactions, level-dependent coupling, and relaxation in a model suitable for quantum dots, molecules, and short nanotubes. We find super-Poissonian shot noise in a bias region where the electronic current is suppressed due to blocking effects. Relaxation due to bosonic excitations has a strong impact on both current and shot noise in this region, for example, the shot noise behaves nonmonotonically as a function of the coupling strength to the bosonic bath. The Fano factor (noise-to-current ratio) can become arbitrarily large in the blocking regime. In another special set of couplings the Fano factor can be reduced to $1/3$, resembling that of a one-dimensional wire.

ACKNOWLEDGMENTS

We enjoyed interesting and helpful discussions with G. Kiesslich as well as financial support by the DFG via the Center for Functional Nanostructures and the Emmy-Noether program.

[1] *Molecular Electronics II*, edited by A. Aviram, M. Ratner, and V. Mujica, Ann. N.Y. Acad. Sci. **960** (2002).
[2] J. Chen, M. A. Reed, A. M. Rawlett, and J. M. Tour, Science **286**, 1550 (1999).
[3] D. Goldhaber-Gordon, H. Shtrikman, D. Mahalu, D. Abusch-Magder, U. Meirav, and M. A. Kastner, Nature (London) **391**, 156 (1998).
[4] J. Park, A. N. Pasupathy, J. I. Goldsmith, C. Chang, Y. Yaish, J. R. Petta, M. Rinkoski, J. P. Sethna, H. D. Abruna, P. L. McEuen, and D. C. Ralph, Nature (London) **417**, 722 (2002).
[5] J. Reichert, H. B. Weber, M. Mayor, and H. v. Löhneysen, Appl. Phys. Lett. **82**, 4137 (2003).
[6] J. Nygard, D. H. Cobden, and P. E. Lindelof, Nature (London) **408**, 342 (2000).
[7] M. R. Buitelaar, T. Nussbaumer, and C. Schönenberger, Phys. Rev. Lett. **89**, 256801 (2002).
[8] P. Jarillo-Herrero, S. Sapmaz, C. Dekker, L. P. Kouwenhoven, and H. S. J. van der Zant, Nature (London) **429**, 389 (2004).
[9] J. Reichert, Ph.D. thesis, Karlsruhe, 2003.
[10] Ya. M. Blanter and M. Büttiker, Phys. Rep. **336**, 1 (2000).
[11] G. Kiesslich, A. Wacker, E. Schoell, A. Nauen, F. Hohls, and R. J. Haug, Phys. Status Solidi C **0**, 1293 (2003).
[12] A. Thielmann, M. H. Hettler, J. König, and G. Schön, Phys. Rev. B **68**, 115105 (2003).
[13] G. Kiesslich, A. Wacker, and E. Schoell, Phys. Rev. B **68**, 125320 (2003).
[14] M. H. Hettler, H. Schoeller, and W. Wenzel, Europhys. Lett. **57**, 571 (2002); in *Nano-Physics and Bio-Electronics: A New Odyssey*, edited by T. Chakraborty, F. Peeters, and U. Sivan (Elsevier, New York, 2002).
[15] J. Weis, R. J. Haug, K. v. Klitzing, and K. Ploog, Phys. Rev. Lett. **71**, 4019 (1993).

[16] F. Cavaliere, A. Braggio, J. T. Stockburger, M. Sassetti, and B. Kramer, Phys. Rev. Lett. **93**, 036803 (2004).
[17] G. Michalek and B. R. Bulka, Eur. Phys. J. B **28**, 121 (2002).
[18] S. S. Safonov, A. K. Savchenko, D. A. Bagrets, O. N. Jouravlev, Y. V. Nazarov, E. H. Linfield, and D. A. Ritchie, Phys. Rev. Lett. **91**, 136801 (2003).
[19] H. Sprekeler, G. Kiesslich, A. Wacker, and E. Schoell, Semicond. Sci. Technol. **19**, 37 (2004).
[20] W. Song, E. E. Mendez, V. Kuznetsov, and B. Nielsen, Appl. Phys. Lett. **82**, 1568 (2003).
[21] M. H. Hettler, W. Wenzel, M. R. Wegewijs, and H. Schoeller, Phys. Rev. Lett. **90**, 076805 (2003).
[22] D. Boese and H. Schoeller, Europhys. Lett. **54**, 668 (2001).
[23] A. Mitra, I. Aleiner, and A. J. Millis, Phys. Rev. B **69**, 245302 (2004).
[24] J. König, H. Schoeller, and G. Schön, Phys. Rev. Lett. **76**, 1715 (1996); J. König, J. Schmid, H. Schoeller, and G. Schön, Phys. Rev. B **54**, 16 820 (1996); H. Schoeller, in *Mesoscopic Electron Transport*, edited by L. L. Sohn, L. P. Kouwenhoven, and G. Schön (Kluwer, Dordrecht, 1997); J. König, *Quantum Fluctuations in the Single-Electron Transistor* (Shaker, Aachen, 1999).
[25] S. Hershfield, J. H. Davies, P. Hyldgaard, C. J. Stanton, and J. W. Wilkins, Phys. Rev. B **47**, 1967 (1993).
[26] A. N. Korotkov, Phys. Rev. B **49**, 10 381 (1994).
[27] The symbolic MAPLE code implementing the computation of the noise via the various matrices is available on request via e-mail to hettler@int.fzk.de
[28] The chosen energy values are appropriate for a quantum dot or short nanotube. For molecules, one would expect energies that are a factor of 100–1000 larger (roughly, meV$\rightarrow$eV).
[29] E. V. Sukhorukov, G. Burkard, and D. Loss, Phys. Rev. B **63**, 125315 (2001).
[30] A. Cottet and W. Belzig, Europhys. Lett. **66**, 405 (2004).
[31] B. R. Bulka, Phys. Rev. B **62**, 1186 (2000); A. Cottet, W. Belzig, and C. Bruder, Phys. Rev. Lett. **92**, 206801 (2004); Phys. Rev. B **70**, 115315 (2004).
[32] C. W. Beenakker and M. Büttiker, Phys. Rev. B **46**, 1889 (1992).
[33] K. E. Nagaev, Phys. Lett. A **169**, 103 (1992).